DOI 10.1002/pmic.200800354 *Proteomics* 2009, *9,* 1274–1292

RESEARCH ARTICLE

Preliminary quantitative profile of differential protein expression between rat L6 myoblasts and myotubes by stable isotope labeling with amino acids in cell culture

Ziyou Cui[1, 2, 3], Xiulan Chen[1, 2]*, Bingwen Lu[4], Sung Kyu Park[4], Tao Xu[4], Zhensheng Xie[1], Peng Xue[1], Junjie Hou[1, 2], Haiying Hang[5], John R. Yates[4]III** and Fuquan Yang[1]*

[1] Proteomics Platform, Institute of Biophysics, Chinese Academy of Sciences, Beijing, China
[2] Graduate University of Chinese Academy of Sciences, Beijing, China
[3] Medical College of CAPF, Tianjin, China
[4] Department of Chemical Physiology, The Scripps Research Institute, La Jolla, CA, USA
[5] Center for Infection and Immunity, Institute of Biophysics, Chinese Academy of Sciences, Beijing, China

Defining the mechanisms governing myogenesis has advanced in recent years. Skeletal-muscle differentiation is a multi-step process controlled spatially and temporally by various factors at the transcription level. To explore those factors involved in myogenesis, stable isotope labeling with amino acids in cell culture (SILAC), coupled with high-accuracy mass spectrometry (LTQ-Orbitrap), was applied successfully. Rat L6 cell line is an excellent model system for studying muscle myogenesis *in vitro*. When mononucleate L6 myoblast cells reach confluence in culture plate, they could transform into multinucleate myotubes by serum starvation. By comparing protein expression of L6 myoblasts and terminally differentiated multinucleated myotubes, 1170 proteins were quantified and 379 proteins changed significantly in fully differentiated myotubes in contrast to myoblasts. These differentially expressed proteins are mainly involved in inter-or intracellular signaling, protein synthesis and degradation, protein folding, cell adhesion and extracelluar matrix, cell structure and motility, metabolism, substance transportation, etc. These findings were supported by many previous studies on myogenic differentiation, of which many up-regulated proteins were found to be involved in promoting skeletal muscle differentiation for the first time in our study. In summary, our results provide new clues for understanding the mechanism of myogenesis.

Received: April 22, 2008
Revised: September 15, 2008
Accepted: September 26, 2008

Keywords:
2D-LC-LTQ-Orbitrap / Quantitative proteomics / SILAC / Skeletal-muscle differentiation

1 Introduction

Skeletal-muscle differentiation is a complicated process coordinated by several transcription factors [1, 2]. Under the control of those transcription factors, proliferating myoblasts withdraw from the cell cycle, and then elongate, adhere, and fuse into multinucleated myotubes. Finally, matured myotubes convert into myofibers, which are capable of muscle contraction. A number of muscle differentiation factors have been discovered such as the myogenic regulatory factors (MRF) and the myocyte enhancer-binding factors (MEF). The expression of these transcription factors, such as MyoD, myogenin, Myf5 and Mef2, is controlled positively by the

Correspondence: Professor Fuquan Yang, Proteomics Platform, Institute of Biophysics, Chinese Academy of Sciences, Beijing 100101, China
E-mail: fqyang@sun5.ibp.ac.cn
Fax: +86-10-6488-8581

Abbreviation: **SILAC,** stable isotope labeling with amino acids in cell culture

* These authors contribute to this work equally.
** Additional corresponding author: Professor John R. Yates, E-mail: jyates@scripps.edu

P38/MAPK, Wnt and Sonic hedgehog (Shh) pathways, and are inhibited by BMP and the Notch/Delta pathway in muscle precursors [1, 3]. When the positive regulation factors are dominant, the transcriptions of muscle-specific genes are activated and the differentiation process is initiated. Although the main factors orchestrating skeletal-muscle differentiation are well defined, little is known about how these growth factors and signal pathways act on myogenic differentiation synergistically [1–3]. When myoblasts proliferate to skeletal cells, many characteristics, from the morphological to the conformational, change significantly. It is reasonable to speculate that many additional cellular components are involved in myogenesis. Accumulating evidences suggest that myogenesis was regulated spatio-temporally by many cellular components; therefore, identifying additional components underlying networks that promote skeletal-muscle differentiation could lead to new insights into the process of myogenesis.

Quantitative proteomics allows measurement of differential protein expression [4, 5]. Tannu *et al.* [6] examined total cellular proteins, membrane-, and nuclear-enriched proteins using 2-DE between proliferating mouse myoblasts of C2C12 cells and fully differentiated myotubes. The proteins they identified are mainly involved in cell signaling, cell cycle and cell shape in differentiating C2C12 cells. Gonnet and colleagues [7] identified 105 proteins with expressional variance in differentiating human myoblasts at different myogenic period by 2D dialysis-assisted gel electrophoresis (DAGE). They found that some unique proteins might participate in human muscle differentiation. Kislinger *et al.* [8] used a gel-free shotgun proteomics method together with label-free quantitative proteomics to profile expression changes in crude nuclei during differentiation stages. Hierarchical clustering of the resulting protein profiles and gene expression found that several types of proteins might be involved in myogenic process, such as integrin, septin. Overall, these studies have presented more information in principle about the characterization of skeletal muscle differentiation by proteomics methods, but hard work on myogenesis still needs to be done because of the very complex myogenic process. Moreover, there are many divergences amongst the previous studies based on molecular methods or proteomics methods. To further discover additional information about the differentiation process, we sought to use stable isotope labeling methods together with shotgun proteomics to quantitate protein expression. Stable isotope labeling with amino acids in cell culture (SILAC) has been combined with highly sensitive MS/MS to create a simple, straightforward, and efficient approach for large-scale protein quantification [5, 9, 10]. SILAC relies on metabolic incorporation of a ''light'' or ''heavy'' isotopic form of the amino acid into cellular proteins [9]. SILAC have been applied in various biological fields to detect the biological changes of protein abundance, protein modification states, and protein-protein interactions [10]. Ong and colleagues [9] used the myogenic differentiation of C2C12 cells as a model to establish and confirm the SILAC method, but they did not present the myogenesis-related proteins in details. In this study, we employed SILAC method with 2D-LC and LTQ-Orbitrap Hybrid Mass Spectrometer to determine protein expression differences between rat L6 myoblasts and myotubes for the first time.

2 Materials and methods

2.1 Materials

Analytical grade chemicals were obtained from Sigma (St. Louis, MO). Milli-Q water was used unless otherwise mentioned. Normal high glucose DMEM media, FBS, glutamine, sodium pyruvate, PBS, penicillin and streptomycin were purchased from Invitrogen (Carlsbad, CA). DMEM deficient in arginine was purchased from JRH Biosciences (Lenexa, KA). Dialyzed FBS was purchased from Biological Industries (Kibbutz Beit Haemek, Israel). Both light $^{12}C_6$ $^{14}N_4$ L-arginine and heavy $^{13}C_6$ $^{15}N_4$ L-arginine were obtained from Spectra Stable Isotopes (Columbia, KS). Protease inhibitor cocktail tablets were obtained from Roche (Basel, Switzerland). Sequence grade trypsin was purchased from Promega (Madison, WI). HPLC-grade ACN, methanol, and formic acid were obtained from J. T. Baker (Phillipsburg, PA). Primary antibodies to tubulin-β, MyoD, desmin, 14-3-3γ, prohibitin-2, and HRP-conjugated secondary antibodies were purchased from Abcam (Cambridge, UK). HRP-conjugated primary antibody to GADPH was purchased from Kangcheng (Shanghai, China). SuperSignal® west Femto trial kit was obtained from Pierce (Rockford, IL).

2.2 Cell culture and isotopic metabolic labeling

Rat L6 myoblasts were maintained in DMEM with 4 mM L-glutamine, 4.5 g/L glucose, 50 UI/mL Penicillin and 50 μg/mL streptomycin, additionally supplemented with 10% v/v FBS (growth medium, GM). Once myoblasts reached confluence, differentiation was induced by lowering the serum concentration to 2% (differentiation medium, DM). For Western blot, L6 myoblasts in common media were subcultured into six 100-mm culture plates. After differentiation was induced, media were changed every 48h. At days 0, 1, 2, 3, 4, and 8, one plate of cells was washed by cold PBS separately and kept at −80°C for protein extraction later. For isotopic metabolic labeling, newly subcultured L6 cells were transferred into DMEM supplemented with 8% dialyzed FBS plus 2% normal FBS and light $^{12}C_6$ $^{14}N_4$ L-arginine or heavy $^{13}C_6$ $^{15}N_4$ L-arginine instead of common GM. L6 myoblasts in light media were induced into myotubes. L6 myoblasts were subcultured in heavy $^{13}C_6$ $^{15}N_4$ L-arginine for at least seven population doublings. Light myotubes and heavy myoblasts were washed three times with ice-cold PBS separately for protein extraction.

2.3 Protein extraction

The process of protein extraction for either MS analysis or Western blot is same. The following steps were carried out at 4°C. Cells were scraped into 8 M urea with protease inhibitor cocktail tablet (Roche, Basel, Switzerland) and sonicated for cells lysis separately. After centrifugation for 30 min at $20\,000 \times g$ in a bench-top centrifuge (Thermo Fisher Scientific, Waltham, MA), the supernatants were collected and kept at −80°C for analysis. Protein concentrations were measured using the Bradford method.

2.4 In-solution digestion

Extracted protein samples from heavy myoblasts and light myotubes were combined at a 1:1 ratio. In-solution digestion was performed with the following protocol. Briefly, 100 μg of protein mixture was dissolved in 8 M urea and 25 mM NH_4HCO_3, reduced with 10 mM DTT for 1 h, alkylated by 40 mM iodoacetamide in the dark for 45 min at room temperature, and then 40 mM DTT was added to quench the iodoacetamide for 30 min at room temperature. After diluting 8 M urea with 25 mM NH_4HCO_3 to 1.6 M, sequence-grade trypsin was added at a ratio of 1:30 and digested at 37°C for overnight. Tryptic digestion was stopped by adding formic acid to a 1% final concentration.

2.5 2D-LC-MS/MS analysis

Digests were centrifuged at $16\,000 \times g$ for 10 min prior to analysis. The supernatant was analyzed by 2D-LC on an LTQ Orbitrap XL (Thermo Fisher Scientific, Waltham, MA) following the method below [11]. For single analyses, 100 μg of peptide mixtures was pressure-loaded onto a 2-D silica capillary column packed with 3 cm of C18 resin (Synergi 4 μm Hydro-RP 80A, Phenomenex, CA) and 3 cm of strong cation exchange resin (Luna 5 μm, SCX 100A, Phenomenex). The buffer solutions used were 5% ACN/0.1% formic acid (buffer A), 80% ACN/0.1% formic acid (buffer B), and 500 mM ammonium acetate/5% ACN/0.1% formic acid (buffer C). The 2-D column was first desalted with buffer A and then eluted using a ten-step salt gradient ranging from 0 to 500 mM ammonium acetate. The effluent of the two-phase column in each case was directed onto a 10-cm C18 analytical column (100-μm id) with a 3-5 μm spray tip. Step 1 consisted of a 100-min gradient from 0–100% buffer B. Steps 2–9 had the following profile: 3 min of 100% buffer A, 3 min of X% buffer C, a 10-min gradient from 0–15% buffer B, and a 97-min gradient from 15–55% buffer B. The 3-min buffer C percentages (X) were 5, 10, 15, 20, 30, 40, 55, and 75%, respectively, for the 8-step analysis. The final step, the gradient contained: 3 min of 100% buffer A, 20 min of 100% buffer C, a 10-min gradient from 0–15% buffer B, and a 107-min gradient from 15–70% buffer B. Nano-ESI was accomplished with a spray voltage of 2.5 kV and a heated capillary temperature of 230°C. A cycle of one full-scan mass spectrum (400–2000 m/z) followed by six data-dependent MS/MS spectra was repeated continuously throughout each salt step of the multidimensional separation. All MS/MS spectra were collected using normalized collision energy (a setting of 35%), an isolation window of 3 m/z, and 1 micro-scan. Application of mass spectrometer scan functions and HPLC solvent gradients were controlled by the XCalibur data system (Thermo Fisher).

2.6 Data analysis and bioinformatics

MS and MS/MS spectra were extracted from the XCalibur data system format (.RAW) into MS1 and MS2 formats by RAW_Xtractor [12]. The target database was the EBI-IPI rat database; sequences for common contaminants such as keratins, IgG, protease autolysis products are added to the database; the whole database (target + contaminants) was then reversed and attached. The MS/MS spectra were interpreted by SEQUEST using an EBI-IPI rat database (Version 3.17, 2006). Results were filtered, sorted, and displayed using the DTASelect2 program [13]. Only peptides with ≥95% confidence score and a ΔCn score of ≥0.1 were considered. In addition, a minimum sequence length of seven-amino acid residues was required. The false positive rate for protein identification was kept below 1%. Quantitative ratios were determined by the software Census version 0.9 [14]. The annotations of proteins were obtained from Swiss-Prot and TrEMBL protein database. For proteins without descriptions, annotations was done by searching the IPI, Swiss-Prot and TrEMBL protein database with BlastP for homologous proteins with descriptions. The PANTHER classification system was used for protein sorting (www.pantherdb.org) with slight modification where a few protein groups with similar annotation were combined. The STRING (http://string.embl.de/), a protein interaction prediction system, was used to retrieve protein associations.

2.7 Western blotting

L6 cells were washed three times with cold PBS and protein was extracted as described above. Equivalent amounts of protein (10 μg/lane) were separated by SDS-PAGE and electroblotted onto 0.45-μm HybondTM-P PVDF membranes (GE healthcare, Piscataway, NJ) by the semi-dry method. Binding of nonspecific proteins to membranes was blocked by incubating these membranes in blocking buffer consisting of 5% non-fat milk in TBS plus 0.05% Tween 20 (TBST) for 1 h at 25°C. Membranes were then incubated at 4°C overnight with primary antibodies diluted in blocking buffer. Membranes were washed three times with TBST, incubated with HRP-conjugated secondary antibodies for 1 h, and then washed three times again with TBST. Finally, immunoreactive proteins on the membranes were detected by SuperSignal® west Femto trial kit and exposed to X-ray film. West-

ern blots were scanned and gray scales were quantified by ImageQuant TL (GE healthcare). L6 cells cultured for Western blotting were harvested three times. Western blotting for every selected protein was repeated three times for every batch of total protein extract.

3 Result and discussion

3.1 Morphological conversion of L6 cells

Rat L6 cell is an excellent model system for developmental biology associated with cell proliferation, signal transduction and cell fate determination. Normally, L6 myoblast cells were cultured in DMEM media supplemented with 10% FBS. In our experiments, with FBS decreasing from 10 to 2% in DMEM media, mononucleate L6 myoblasts in good conditions fused and transformed into multinucleate myotubes very quickly. One day later after serum deprivation, myocytes are scattered in the cell culture plate. In spite of that, the shapes of L6 cells were distinct from myoblasts. After 2 days, about 35% area of culture plate was occupied by myocytes. After 3 days, more than 85% of cells have fused into elongated myotubes. At the end of day 4, giant elongated multinucleate myotubes have outspread apparently everywhere on the culture plate. As shown in Fig. 1, the morphology of cells from myoblasts to myotubes has changed significantly. Accompanied with the morphological conversion of myoblast into myotubes, some muscle-specific proteins were expressed at high level in myotubes comparing with myoblasts. We examined muscle-differentiation marker proteins desmin and MyoD by Western blot (Fig. 2A). As the Fig. 2A showed, the expressional levels of these marker proteins were increased gradually during myogenic process but decreased in D8 myotubes. In addition, our SILAC results show that some other muscle-differentiation markers, such as myosin heavy chain (MHC), skeletal muscle actin alpha, and myosin heavy polypeptide 2, also were up-regulated during myogenic process. In conclusion, L6 myoblasts had well differentiated into myotubes.

3.2 Protein identification and quantification

The morphological conversion of L6 cells from myoblasts to myotubes is presumed to be driven by proteins that follow tissue- and cell-specific expression. The goal of this work was to find expression differences between rat L6 myoblasts and myotubes. The tryptic peptides were analyzed by 2D-LC-LTQ-Orbitrap MS system [11]. For protein identification, a decoy database was used and the false positive rate for protein identification was kept below 1% in this study. After filtering with stringent parameters, 12 729 peptides and 2767 proteins were identified from all experiments (see Supporting Information Table 1). Among these proteins, 1170 were quantified with high confidence (see Supporting Informa-

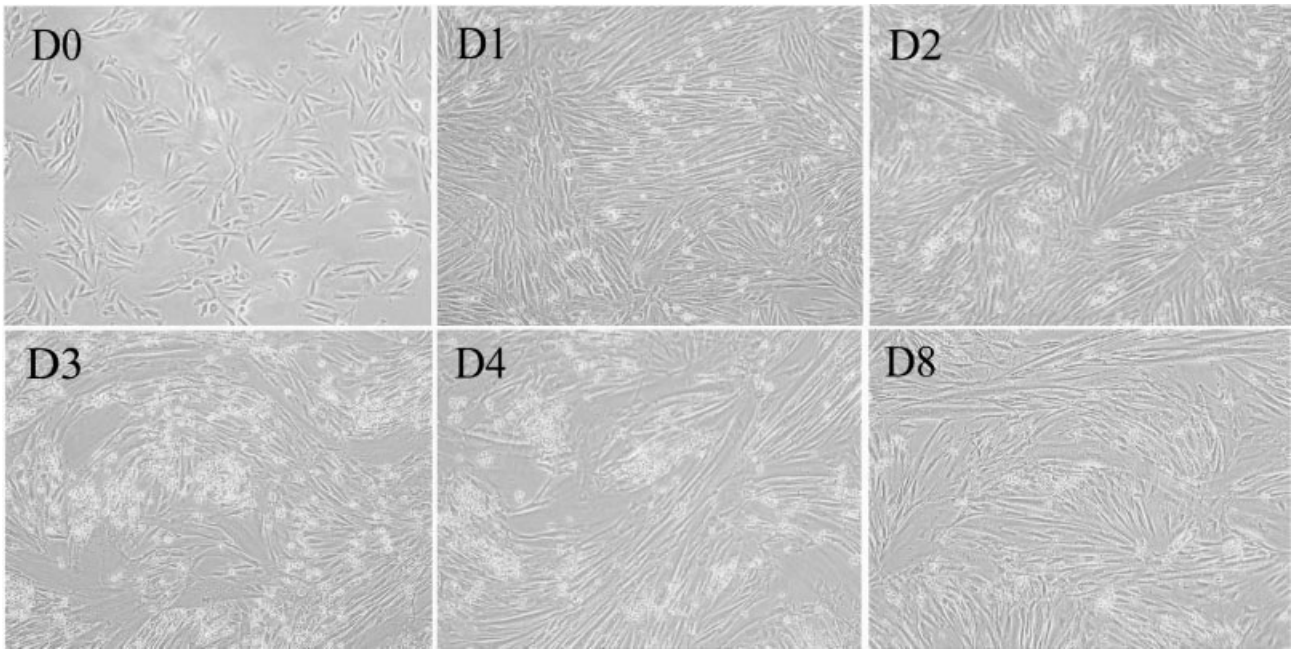

Figure 1. The light micrographs of cultured L6 cells were enlarged by 10*10. D0 represents that the myoblasts before differentiation initiation were grown in DMEM supplemented with 10% FBS. D1, D2, D3 and D4 indicate that L6 cells have been cultured in DMEM with 2% FBS for 1, 2, 3 and 4 days, respectively. D4 were fully differentiated myotubes. D8 indicates myotubes have been serum-starved for another 4 days starting from D4.

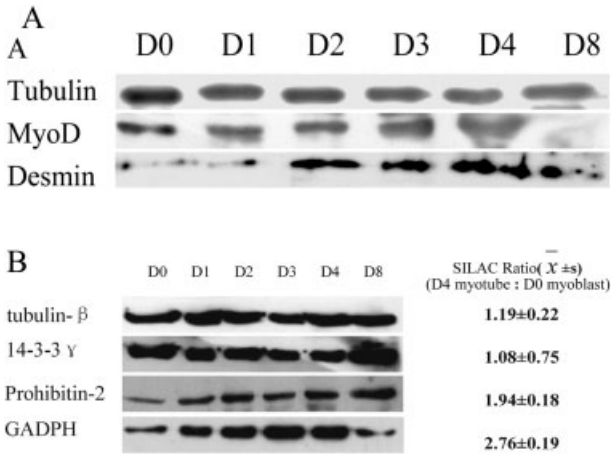

Figure 2. Western blotting. (A) Western blotting of L6 differentiation marker or differentiation associated proteins in L6 blasts to L6 myotubes. (B) Validation of SILAC ratio by Western blotting.

tion Tables 1 and 2); 780 proteins (about 67%) were quantified with two or more peptides (see Supporting Information Fig. 1). Among the quantified proteins, 342 proteins were up-regulated (≥1.5-fold changes, see Table 1) and 37 proteins were down-regulated (≤0.5-fold changes) in fully differentiated myotubes (see Table 2). The remaining proteins were considered as no significant changes (see Supporting Information Table 1). Our results show that the expression of many conserved proteins, such as tubulin β chain, tubulin β 2, tubulin β 5 and actin β (actin, cytoplasmic 1), remained stable, suggesting the accuracy of the quantitative results in our experiment to some extent. To further validate the accuracy of the quantitative results by different methods, several proteins with different SILAC quantitative ratio were quantified again by Western blotting. Figure 3 shows that the results of Western blotting for tubulin-β, 14-3-3γ, prohibitin-2 and GADPH are strongly consistent with the quantitative results determined by MS.

3.3 The comparative profiling of protein expression

Many of the differentially expressed proteins observed in this study have been reported to be involved in myogenic regulation, and some were newly discovered in this study.

Proteins increased in expression (ratio ≥1.5) were sorted by the PANTHER classification system (Fig. 3 and Table 1). These proteins are mainly involved in inter-or intracellular signaling, protein synthesis and protein degradation, protein

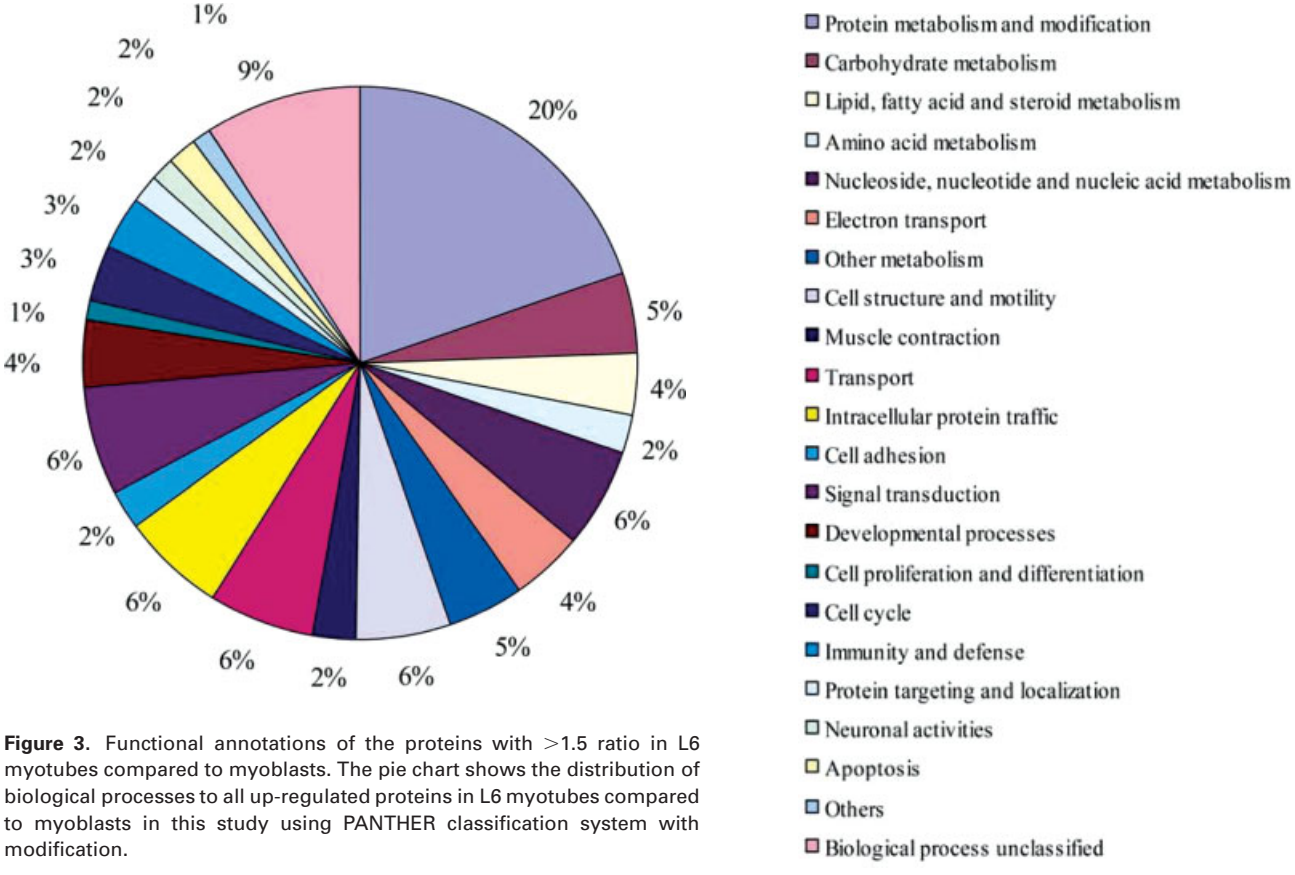

Figure 3. Functional annotations of the proteins with >1.5 ratio in L6 myotubes compared to myoblasts. The pie chart shows the distribution of biological processes to all up-regulated proteins in L6 myotubes compared to myoblasts in this study using PANTHER classification system with modification.

Table 1. Classification of proteins with the ratio ≥1.5

Description	IPI ID	Average ratio Average±SD	Quantification Peptide Num	UniProtKB ID/AC	Gene ID
Mediators of signaling pathway					
Dual specificity mitogen-activated protein kinase 1 (MAPKK 1)	IPI00231247.8	1.75±NA	1	Q01986	170851
Guanine nucleotide-binding protein G(i), alpha-2 subunit	IPI00231925.7	1.79±0.01	3	P04897	81664
Hypothetical protein LOC361120	IPI00364617.2	1.53±NA	1	Q4QQT7	361120
Inositol 1,4,5-trisphosphate receptor type 3(IP3R-3)	IPI00206986.1	1.55±NA	1	Q63269	25679
latent transforming growth factor beta binding protein 1	IPI00389331.1	1.80±0.00	2	Q00918	59107
Membrane associated progesterone receptor component 2	IPI00373197.1	2.15±0.15	2	Q5XIU9	361940
Phosphatidylethanolamine-binding protein	IPI00230937.4	1.62±NA	1	P31044	29542
PREDICTED: A kinase (PRKA) anchor protein 2	IPI00364858.3	4.05±NA	1	Q5U301	298024
PREDICTED: similar to Dual specificity protein phosphatase 3	IPI00568511.1	1.95±NA	1		498003
PREDICTED: similar to mitogen-activated protein kinase 4 isoform (Map4k4)	IPI00357885.3	2.28±NA	1		301363
PREDICTED: similar to Ran-binding protein 10	IPI00365184.2	1.87±NA	1		361396
PREDICTED: similar to receptor expression enhancing protein 5	IPI00360246.2	3.34±0.22	2		364838
PREDICTED: similar to Semaphorin 3C	IPI00372650.3	1.88±NA	1		296787
Prenylated Rab acceptor protein 1	IPI00208565.1	2.18±NA	1	O35394	83583
Prohibitin-2	IPI00190557.2	1.94±0.18	4	Q5XIH7	114766
RAB10, member RAS oncogene family	IPI00555185.1	2.18±0.02	3	Q5RKJ9	50993
Ras-related protein Rab-2A	IPI00202570.1	1.50±NA	1	P05712	65158
Reticulocalbin 3, EF-hand calcium binding domain	IPI00207050.5	55.97±NA	1	Q63399	494125
SH2-containing inositol phosphatase 2	IPI00205291.1	3.02±1.10	2	Q9WVR3	65038
Signal sequence receptor, alpha	IPI00561555.1	1.78±NA	1	Q4V7D1	361233
Splice Isoform 3 of Protein kinase C and casein kinase substrate in neurons 2 protein	IPI00231216.1	1.55±NA	1	Q9QY17	124461
Striatin, calmodulin binding protein 3	IPI00476338.2	2.37±0.19	4	P58405	114520
Translocon-associated protein gamma subunit	IPI00196589.2	1.67±NA	1	Q08013	81784
A-kinase anchor protein 11	IPI00210194.1	1.84±NA	1	Q62924	498549
Protein synthesis					
3-hydroxyisobutyrate dehydrogenase, mitochondrial precursor	IPI00202658.1	2.05±NA	1	P29266	63938
60S ribosomal protein L5	IPI00230914.4	3.83±3.73	5	P09895	81763
Asparaginyl-tRNA synthetase	IPI00421313.1	1.99±0.27	7	Q6TUD1	291556
Cc2-5	IPI00382192.1	4.16±NA	1	Q7TP13	307759
Dolichyl-diphosphooligosaccharide–protein glycosyltransferase 63 kDa subunit precursor	IPI00188059.2	1.65±0.05	3	P25235	64701
Elongation factor 1-alpha 1	IPI00195372.1	1.58±0.04	13	P62630	171361
Elongation factor 2	IPI00203214.5	1.61±0.10	18	P05197	29565
ERGIC-53 protein precursor	IPI00210116.2	1.54±0.06	3		116666
Eukaryotic translation elongation factor 1 delta	IPI00471525.2	2.07±0.07	8	Q68FR9	300033
Eukaryotic translation initiation factor 2 subunit 1	IPI00230830.4	1.73±NA	1	P68101	54318
Eukaryotic translation initiation factor 3 subunit 9	IPI00363771.3	1.50±0.06	6	Q4G061	288516
Eukaryotic translation initiation factor 4A2	IPI00193595.3	2.07±0.96	7	Q52KC1(m)	303831
GERp95	IPI00214529.3	1.91±NA	1	Q9QZ81	59117
Glutamyl-prolyl-tRNA synthetase	IPI00421357.2	1.98±0.32	3	Q6TXE9	289352
Hypothetical protein LOC619440	IPI00201819.1	1.64±0.05	2	Q5XI97	619440
IKIP1 protein	IPI00199778.1	1.62±0.05	3	Q5EAJ6	314730
Leucine rich repeat containing 47 (predicted)	IPI00359172.1	2.00±0.00	2		362672
Leucyl-tRNA synthetase	IPI00363236.2	1.57±NA	1	Q5PPJ6	291624

Table 1. Continued

Description	IPI ID	Average ratio Average±SD	Quantification Peptide Num	UniProtKB ID/AC	Gene ID
Phenylalanine-tRNA synthetase-like, beta subunit	IPI00202379.1	1.71±0.31	3	Q68FT7	301544
PREDICTED: eukaryotic translation elongation factor 1 gamma	IPI00470317.3	3.04±0.03	2	Q68FR6	293725
PREDICTED: similar to Eif3s1 protein	IPI00364189.1	1.50±0.10	2	A0JPM9	311371
PREDICTED: similar to Eukaryotic translation elongation factor 1 beta 2	IPI00476899.1	2.45±NA	1		363241
PREDICTED: similar to eukaryotic translation initiation factor 3, subunit 10 theta, 150/170kDa	IPI00372810.2	1.59±0.11	2	Q4G020	292148
PREDICTED: similar to Glycyl-tRNA synthetase	IPI00364262.2	1.90±0.06	3	Q5I0G4	297113
PREDICTED: similar to isoleucine-tRNA synthetase	IPI00365783.3	2.04±NA	1	Q6NXK4(m)	306804
PREDICTED: similar to Methionine-tRNA synthetase	IPI00366397.2	1.71±0.00	2		299851
PREDICTED: similar to Mitochondrial 28S ribosomal protein S30	IPI00214903.3	1.66±NA	1	Q9D0G0(m)	294767
PREDICTED: similar to Signal recognition particle 68	IPI00368134.2	1.63±0.24	2		363707
PREDICTED: similar to Tryptophanyl-tRNA synthetase	IPI00365914.2	2.40±0.02	3	Q6P7B0	314442
PREDICTED: similar to Tu translation elongation factor, mitochondrial	IPI00371236.2	1.56±0.00	2		293481
Probable ATP-dependent RNA helicase DDX46	IPI00208266.2	1.59±NA	1	Q62780	245957
Prolyl 4-hydroxylase alpha-1 subunit precursor	IPI00209863.2	1.97±0.26	2	P54001	64475
Prolyl 4-hydroxylase alpha-2 subunit precursor	IPI00372370.2	1.77±0.00	2		360526
Ribophorin I	IPI00204365.2	1.63±0.10	5	Q6P7A7	25596
Seryl-aminoacyl-tRNA synthetase 1	IPI00373410.3	2.40±0.09	4	Q6P799	266975
Syntaxin 12	IPI00208759.2	1.74±NA	1	O88385	65033
Threonyl-tRNA synthetase, cytoplasmic	IPI00559880.1	1.98±0.04	3	Q5XHY5	294810
Transcriptional activator protein Pur-beta	IPI00189358.2	3.76±0.80	3	Q68A21	498407
Transitional endoplasmic reticulum ATPase	IPI00212014.2	1.50±0.13	13	P46462	116643
Tyrosyl-tRNA synthetase	IPI00366785.2	1.66±NA	1	Q4KM49	313047
WD repeat domain 77	IPI00368916.1	1.59±NA	1	Q4QR85	310769
Proteolysis					
26S protease regulatory subunit 4	IPI00211733.1	1.88±NA	1	P62193	117263
26S protease regulatory subunit 7	IPI00421600.7	1.78±0.10	4	Q63347	25581
ATPase family AAA domain-containing protein 1	IPI00566676.1	1.55±NA	1		309532
Dipeptidyl-peptidase 2 precursor	IPI00230946.4	3.14±NA	1	Q9EPB1	83799
Fxna	IPI00390597.2	1.73±NA	1	Q6UPR8	373544
Insulin-like growth factor binding protein 5 protease	IPI00199325.1	4.11±0.24	4	Q9QZK5	65164
Lon	IPI00205076.1	2.19±0.01	3	Q924S5	170916
Midline-1	IPI00231578.4	2.65±NA	1	P82458	54252
Mitochondrial-processing peptidase beta subunit, mitochondrial precursor	IPI00209980.5	2.35±NA	1	Q03346	64198
PREDICTED: aminopeptidase puromycin sensitive	IPI00372700.1	2.22±0.15	5	Q8VID2	50558
PREDICTED: proteasome (prosome, macropain) subunit, beta type 5	IPI00230992.4	2.50±NA	1	Q91X53	29425
PREDICTED: similar to 26S proteasome non-ATPase regulatory subunit 11	IPI00370382.1	1.52±0.03	3	Q8BG32	303353
PREDICTED: similar to 26S proteasome subunit p40.5	IPI00202283.1	1.58±0.49	2	Q9WVJ2	365388
PREDICTED: similar to Expressed sequence AI314180	IPI00367234.2	1.76±0.08	3		313196
PREDICTED: similar to HECT domain containing 1	IPI00365611.2	1.97±NA	1		362736
PREDICTED: similar to Psmc6 protein	IPI00362105.1	1.82±NA	1	Q32PW9	289990
Prenylcysteine oxidase precursor	IPI00198080.1	1.54±NA	1	Q99ML5	246302
Proteasome (Prosome, macropain) 26S subunit, ATPase 3	IPI00190392.3	1.52±NA	1	Q63569	29677
Proteasome (Prosome, macropain) 26S subunit, non-ATPase, 2 (PSMD2)	IPI00370456.1	1.58±0.19	10	Q4FZT9	287984
Proteasome 26S subunit, non-ATPase, 3	IPI00370009.1	1.56±0.05	5	Q5U2S7	287670

Table 1. Continued

Description	IPI ID	Average ratio Average±SD	Quantification Peptide Num	UniProtKB ID/AC	Gene ID
Proteasome subunit alpha type 1(PSMA1)	IPI00191748.3	1.72±NA	1	P18420	29668
Proteasome subunit alpha type 2	IPI00231757.11	1.77±0.07	3	P17220	29669
Proteasome subunit alpha type 3	IPI00476178.2	4.42±0.01	2	Q6IE67	408248
Proteasome subunit alpha type 4	IPI00231046.8	1.61±0.00	2	P21670	29671
Proteasome subunit alpha type 5	IPI00191502.5	1.50±0.03	5	P34064	29672
Proteasome subunit beta type 1 (PSMB1)	IPI00191749.5	1.64±0.28	3	P18421	94198
Proteasome subunit beta type 2	IPI00188584.1	1.61±0.02	3	P40307	29675
Proteasome subunit beta type 4 precursor	IPI00191505.3	1.60±NA	1	P34067	58854
Proteasome, 26S, non-ATPase regulatory subunit 6	IPI00189463.1	1.70±0.05	4	Q6PCT9	289924
Protective protein for beta-galactosidase	IPI00464785.1	1.91±0.00	2	Q6AYS3	296370
Prothrombin precursor (Fragment)	IPI00189981.1	5.18±NA	1	P18292	29251
Secernin 1	IPI00202627.1	1.83±NA	1	Q6AY84	502776
Tripeptidyl-peptidase 2	IPI00213579.2	1.59±NA	1	Q64560	81815
Ubiquitin-conjugating enzyme E2 variant 2	IPI00339040.2	1.67±0.12	2	Q7M767	287927
Molecular chaperone					
10 kDa heat shock protein, mitochondrial	IPI00326433.10	2.20±0.04	3	P26772	25462
60 kDa heat shock protein, mitochondrial precursor	IPI00339148.2	1.53±0.04	8	P63039	63868
78 kDa glucose-regulated protein precursor	IPI00206624.1	1.75±0.06	13	P06761	25617
Calnexin Precursor	IPI00199636.1	1.76±0.23	8	P35565	29144
Chaperonin subunit 6a	IPI00188111.1	1.50±0.06	6	Q3MHS9	288620
Heat shock 70 kDa protein 4/Ischemia responsive 94 kDa protein	IPI00387868.2	1.83±0.12	3	O88600	266759
Heat shock cognate 71 kDa protein	IPI00208205.1	1.58±0.07	8	P63018	24468
Heat shock protein (HSP) 90-beta	IPI00471584.5	1.50±0.09	9	P34058	301252
Heat-shock protein beta-1	IPI00201586.1	2.55±0.24	4	P42930	24471
Heat-shock protein beta-8	IPI00189624.1	2.09±NA	1	Q9EPX0	113906
Hsc70-interacting protein	IPI00199273.1	1.83±0.05	3	P50503	81800
Hypoxia up-regulated 1	IPI00559738.1	1.94±NA	1	Q63617	192235
Kelch repeat and BTB domain-containing protein 10	IPI00190417.1	9.96±NA	1	Q9ER30	117537
Pincher	IPI00200271.1	3.01±NA	1	Q8R3Z7	192204
PREDICTED: low density lipoprotein Receptor-related protein associated protein 1	IPI00364124.1	1.56±NA	1	Q99068	116565
PREDICTED: similar to CCT eta, eta subunit of the chaperonin containing TCP-1	IPI00364286.2	1.70±0.21	2		297406
T-complex protein 1 subunit alpha	IPI00200847.1	1.51±0.03	3	P28480	24818
Ubiquitin fusion degradation 1-like isoform 1	IPI00195248.4	1.63±NA	1	Q9ES53	84478
Cell-adhesion proteins					
Glypican-1 precursor	IPI00194930.5	1.70±0.12	10	P35053	58920
Integrin beta-1 precursor	IPI00191681.1	2.30±NA	1	P49134	24511
Lactadherin precursor	IPI00188896.1	2.32±0.17	8	P70490	25277
Neural cell adhesion molecule 1, 140 kDa isoform precursor	IPI00476991.1	3.88±NA	1	P13596/ Q3T1H3	24586
PREDICTED: laminin, alpha 5	IPI00190577.4	2.27±NA	1	P70636	140433
PREDICTED: laminin, gamma 1	IPI00363849.2	2.70±NA	1	P97552	117036
PREDICTED: nidogen 2	IPI00372786.3	2.43±0.33	9	Q5M812	302248
PREDICTED: similar to alpha 3 type VI collagen isoform 1 precursor	IPI00360737.2	1.51±0.10	4		367313
PREDICTED: similar to Elastin microfibril interfacer 1	IPI00199867.1	2.83±0.25	7		298845
PREDICTED: similar to laminin B1	IPI00365542.2	1.50±0.05	2		298941
PREDICTED: similar to Transmembrane 4 superfamily member 6	IPI00201753.1	3.18±0.00	2	Q5RJZ3	302313
PREDICTED: similar to type XV collagen	IPI00364868.2	3.21±0.45	4	Q4G024	298069
PREDICTED: similar to Vinculin	IPI00365286.3	1.55±0.12	17	Q9ESQ3	305679
Procollagen C-endopeptidase enhancer 1 precursor	IPI00194566.1	2.44±0.06	4	O08628	29569

Table 1. Continued

Description	IPI ID	Average ratio Average±SD	Quantification Peptide Num	UniProtKB ID/AC	Gene ID
Protein-lysine 6-oxidase precursor	IPI00214661.1	2.56±NA	1	P16636	24914
Splice Isoform 1 of Fibronectin precursor	IPI00200757.1	2.30±0.17	50	P04937	25661
OX-2 membrane glycoprotein precursor(Cd200)	IPI00193967.2	5.26±NA	1	P04218	24560
PREDICTED: similar to Fibulin-1 precursor	IPI00370411.2	1.92±NA	1		315191
PREDICTED: similar to fibulin-2	IPI00388257.3	1.55±0.90	8	Q8CJG7	282583
Cell structure and motility					
Actin, alpha cardiac	IPI00194087.3	1.61±0.13	10	P68035	29275
Actin, alpha skeletal muscle	IPI00189813.1	1.98±1.38	11	P68136	29437
Actin-related protein 2/3 complex subunit 1A	IPI00200845.1	2.19±NA	1	Q6PCU9	81824
Microtubule-associated protein 1S	IPI00362631.1	1.81±NA	1		290640
Double cortin and calcium/calmodulin-dependent protein kinase-like 1	IPI00373202.2	11.43±NA	1	O08875	83825
General vesicular transport factor p115	IPI00324618.3	1.57±0.20	2	P41542	56042
Hypothetical protein RGD1305887	IPI00195673.1	2.09±1.41	15	Q4QQV0	307351
Isoform 1 of Tropomyosin alpha-3 chain(Tpm3)	IPI00372259.4	1.58±0.65	5	Q63610	117557
Kinesin-1 heavy chain	IPI00364904.2	4.43±0.52	10	Q2PQA9	117550
Microtubule-associated protein 1A	IPI00199693.2	1.76±NA	1	P34926	25152
Microtubule-associated protein 4	IPI00393975.2	1.71±0.09	4	Q5M7W5	367171
Microtubule-associated protein RP/EB family member 3	IPI00360288.1	3.35±NA	1	Q5XIT1	298848
Myosin heavy chain, fast skeletal muscle, embryonic	IPI00201578.1	219.81±2.46	4	P1284	24583
Myosin light polypeptide 4	IPI00214457.1	127.46±35.09	5	P17209	688228
Myosin, heavy polypeptide 2, skeletal muscle, adult	IPI00554308.2	443.05±NA	1	Q0GC40	691644
Nestin	IPI00194103.1	7.23±0.84	8	P21263	25491
PREDICTED: similar to cofilin	IPI00369419.2	4.49±NA	1	P45592	366624
PREDICTED: similar to cytoskeleton-associated protein 4	IPI00365982.1	1.66±0.17	6		362859
PREDICTED: similar to gamma-filamin	IPI00358175.2	4.90±0.28	8	Q8VHX6(m)	362332
PREDICTED: similar to microfilament and actin filament cross-linker protein isoform a	IPI00359003.3	3.07±0.48	2		362587
PREDICTED: similar to nebulin	IPI00372072.2	3.43±NA	1		311029
PREDICTED: similar to titin isoform N2-B	IPI00564395.1	7.65±NA	1	P97850	84015
Septin-7	IPI00204899.1	1.52±0.14	4	A2VCW8	64551
Smooth muscle alpha-actin	IPI00197129.1	2.69±3.13	14	Q63030	81633
Spectrin alpha chain, brain	IPI00209258.4	1.57±0.09	18	Q6IRK8	64159
Splice Isoform 1 of Tropomyosin 1 alpha chain	IPI00197888.2	2.06±0.10	3	P04692	24851
Splice Isoform 2 of Tropomyosin beta chain	IPI00187731.4	2.75±0.55	3	P58775	500450
Stomatin (Epb7.2)-like 2	IPI00203528.1	1.80±NA	1	Q4FZT0	298203
Transgelin	IPI00231196.4	4.90±0.00	2	O08564	25123
Vesicle-associated membrane protein-associated protein A	IPI00209290.2	2.25±0.02	5	Q9Z270	58857
Metabolism					
2,4-dienoyl-CoA reductase, mitochondrial precursor	IPI00213659.3	1.94±0.19	3	Q64591	117543
6-phosphofructokinase, muscle type	IPI00231293.6	1.57±NA	1	P47858	65152
Aldose reductase	IPI00231737.4	1.65±0.04	3	P07943	24192
Alpha-enolase	IPI00464815.10	1.60±0.05	11	P04764	24333
Alpha-N-acetylglucosaminidase	IPI00370034.2	2.01±NA	1	Q5XIA5	287711
Annexin A11	IPI00364621.2	1.76±NA	1	Q5XI77	290527
Asparagine synthetase	IPI00471908.5	4.10±NA	1	P49088	25612
Aspartate aminotransferase, cytoplasmic	IPI00421513.6	1.63±NA	1	P13221	24401
ATP synthase alpha chain, mitochondrial precursor	IPI00396910.1	1.93±0.29	5	P15999	65262
ATP synthase B chain, mitochondrial precursor	IPI00196107.1	2.23±0.00	2	P19511	171375
ATP synthase beta chain, mitochondrial precursor	IPI00551812.1	2.08±0.13	22	P10719	171374
ATP synthase delta chain, mitochondrial precursor	IPI00198620.1	2.04±0.05	2	P35434	245965

Table 1. Continued

Description	IPI ID	Average ratio Average±SD	Quantification Peptide Num	UniProtKB ID/AC	Gene ID
ATP synthase D chain, mitochondrial	IPI00230838.4	2.48±0.00	2	P31399	641434
ATP synthase, H+ transporting, mitochondrial F1 Complex, gamma polypeptide 1	IPI00396906.1	2.21±NA	1	Q6PCU0	116550
Beta-hexosaminidase alpha chain precursor	IPI00394353.1	1.74±0.09	3	Q641X3	300757
Beta-hexosaminidase beta chain precursor	IPI00464518.1	1.55±NA	1	Q6AXR4	294673
Biliverdin reductase A precursor	IPI00230874.10	7.20±NA	1	P46844	116599
Citrate synthase	IPI00206977.1	2.10±0.33	2	Q8VHF5	170587
COX15 homolog, cytochrome c oxidase assembly protein	IPI00361315.2	1.74±NA	1	Q3T1G9	309391
Cytochrome c oxidase polypeptide Va, mitochondrial precursor	IPI00192246.1	2.48±0.03	3	P11240	252934
Cytochrome c, somatic	IPI00231864.4	1.90±0.03	3	P62898	25309
D-3-phosphoglycerate dehydrogenase	IPI00475835.2	1.60±0.00	2	O08651	58835
Dihydrolipoamide dehydrogenase	IPI00365545.1	2.64±0.16	2	Q6P6R2	298942
Dihydrolipoamide S-acetyltransferase	IPI00231714.3	1.67±0.66	4	P08461	81654
Electron transfer flavoprotein beta-subunit	IPI00364321.2	1.91±NA	1	Q68FU3	292845
Fructose-bisphosphate aldolase A	IPI00231734.4	3.16±0.10	13	P05065	24189
Fumarate hydratase, mitochondrial precursor	IPI00231611.7	1.91±0.85	4	P14408	24368
Glucose phosphate isomerase	IPI00364311.1	2.09±0.10	4	Q6P6V0	292804
Glucosidase, alpha acid	IPI00400579.1	1.61±0.65	5	Q6P7A9	367562
Glyceraldehyde-3-phosphate dehydrogenase	IPI00212647.2	2.76±0.19	10	P04797	24383
GTP:AMP phosphotransferase mitochondrial	IPI00362243.6	2.38±0.06	2	P29411	26956
Hsd17b4 protein	IPI00326948.2	1.66±0.00	2	Q6IN39	79244
Hypothetical LOC361596	IPI00464897.1	1.53±0.17	4	Q6DGF1	361596
Hypothetical protein LOC360975	IPI00215093.1	1.66±0.08	4	Q5XI78	360975
Isocitrate dehydrogenase [NAD] subunit beta, mitochondrial precursor	IPI00357924.1	1.51±0.25	4	Q68FX0	94173
Lactoylglutathione lyase	IPI00188304.2	1.53±0.01	3	Q6P7Q4	294320
L-lactate dehydrogenase A chain	IPI00197711.1	2.10±0.11	6	P04642	24533
Low molecular mass ubiquinone-binding protein	IPI00382312.3	2.36±NA	1	Q7TQ16	497902
LRRGT00113	IPI00196629.3	2.00±NA	1		499358
Malate dehydrogenase, mitochondrial	IPI00566583.1	2.04±0.09	8		81829
Methylmalonate-semialdehyde dehydrogenase [acylating], mitochondrial precursor	IPI00205018.2	4.11±NA	1	Q02253	81708
Mitochondrial-processing peptidase alpha subunit, mitochondrial	IPI00195551.1	2.06±0.05	3	P20069	296588
N-acylglucosamine 2-epimerase	IPI00204162.1	2.17±0.00	2	P51607	81759
NADH-cytochrome b5 reductase	IPI00231662.5	1.50±0.07	8	P20070	25035
Nicotinamide nucleotide transhydrogenase	IPI00555265.1	1.90±0.26	2	Q5BJZ3	310378
Nucleoside diphosphate kinase A	IPI00194404.5	1.54±0.05	7	Q05982	191575
Peptidase D	IPI00364304.2	1.78±NA	1	Q5I0D7	292808
PREDICTED: dihydrolipoamide branched chain transacylase E2	IPI00373418.3	1.96±0.00	2	Q99PU6	29611
PREDICTED: similar to catechol-O-methyltransferase domain containing 1	IPI00365293.2	1.98±NA	1		305685
PREDICTED: similar to Cox7a2l protein	IPI00365505.2	2.49±NA	1	P28075	316064
PREDICTED: similar to Cytochrome c oxidase polypeptide VIb	IPI00389152.3	1.68±0.11	4		502592
PREDICTED: similar to glyceraldehyde-3-phosphate dehydrogenase	IPI00554039.1	2.78±0.21	10		498099
PREDICTED: similar to phosphoacetylglucosamine mutase	IPI00205603.3	2.80±0.06	2		363109
PREDICTED: similar to pyrroline-5-carboxylate synthetase short isoform	IPI00372524.3	1.52±0.32	9		361755
PRx III (Thioredoxin-dependent peroxide reductase, mitochondrial)	IPI00208215.1	2.01±0.07	3	Q9Z0V6	64371

Table 1. Continued

Description	IPI ID	Average ratio Average±SD	Quantification Peptide Num	UniProtKB ID/AC	Gene ID
Pyruvate dehydrogenase E1 component alpha subunit, somatic form, mitochondrial precursor	IPI00191707.3	4.27±4.91	3	P26284	29554
Pyruvate dehydrogenase E1 component subunit beta, mitochondrial precursor	IPI00194324.1	2.91±1.75	3	P49432	289950
Serum deprivation response protein	IPI00362416.1	3.41±NA	1	Q66H98	316384
Superoxide dismutase [Mn], mitochondrial precursor	IPI00211593.1	1.57±0.00	2	P07895	24787
Trifunctional enzyme alpha subunit, mitochondrial precursor	IPI00212622.1	1.71±0.08	10	Q64428	170670
Trifunctional enzyme beta subunit, mitochondrial precursor	IPI00198467.1	1.66±NA	1	Q60587	171155
Triosephosphate isomerase	IPI00231767.4	3.72±0.91	2	P48500	24849
Ubiquinol-cytochrome c reductase core protein I	IPI00471577.1	2.52±0.36	4	Q68FY0	301011
Ubiquinol-cytochrome c reductase core protein II	IPI00480805.1	2.78±0.54	4	P32551	293448
PREDICTED: similar to cytochrome c-1	IPI00366416.1	2.60±0.56	4		300047
SIALIDASE-1 PRECURSOR.	IPI00201456.5	2.07±NA	1	Q99PW3	24591
Fumarylacetoacetate hydrolase domain-containing protein 1	IPI00368708.2	2.54±NA	1	Q6AYQ8	302980
Long-chain-fatty-acid–CoA ligase 1	IPI00188989.1	4.29±1.17	3	P18163	25288
Phosphoglycerate kinase 1	IPI00231426.5	2.17±0.16	7	P16617	24644
PREDICTED: similar to inosine monophosphate dehydrogenase 1 isoform b	IPI00480747.2	1.72±NA	1		362329
PREDICTED: similar to NADH dehydrogenase (ubiquinone) 1 alpha subcomplex, assembly factor 1	IPI00373108.2	2.44±NA	1		296086
Pyruvate dehydrogenase [lipoamide] kinase isozyme 1, mitochondrial precursor	IPI00204957.1	4.57±NA	1	Q63065	116551
Sulfated glycoprotein 1 precursor	IPI00195160.1	1.72±0.32	2	P10960	25524
Acyl-Coenzyme A thioesterase 2, mitochondrial	IPI00358498.2	1.64±0.00	2	O55171	302640
PREDICTED: similar to myotubularin-related protein 2	IPI00362271.3	1.61±NA	1		315422
PREDICTED: similar to phosphoenolpyruvate carboxykinase 2	IPI00388232.3	1.77±0.43	2		361042
Serine hydroxymethyl transferase 2	IPI00195109.3	1.80±0.08	2	Q5U3Z7	299857
Splice Isoform 1 of Lipid phosphate phospho-hydrolase 1	IPI00193763.1	4.59±NA	1	O08564	64369
Long-chain-fatty-acid–CoA ligase 3	IPI00205908.1	3.25±0.70	3	Q63151	114024
NAD(P)H:quinone oxidoreductase type 3, polypeptide A2	IPI00371971.2	2.29±0.28	2	Q5EB81	304805
PREDICTED: similar to Pyruvate dehydrogenase kinase, isoenzyme 3	IPI00192133.3	1.98±NA	1		296849
Adenylate kinase isoenzyme 4, mitochondrial	IPI00204311.1	6.46±NA	1	Q9WUS0	29223
NADH dehydrogenase subunit 4	IPI00200487.1	1.55±NA	1	P05508	
Acyl-CoA thioesterase 7	IPI00213571.1	1.84±NA	1	Q64559	26759
Dehydrogenase/reductase (SDR family) member 7B	IPI00369545.2	3.09±NA	1	Q5RJY4	287380
11 kDa protein	IPI00390086.2	1.83±NA	1	Q6IBB3(h)	690441
Ubiquinol-cytochrome c reductase complex 11 kDa protein, mitochondrial precursor	IPI00369093.1	2.48±NA	1	Q5M9I5	366448
20 alpha-hydroxysteroid dehydrogenase	IPI00189189.2	23.55±NA	1	Q91XV8	171516
NADH dehydrogenase (Ubiquinone) Fe-S protein 1	IPI00358033.1	1.67±NA	1	Q66HF1	301458
87 kDa protein	IPI00212665.2	1.76±0.12	2		116645
Similar to CG6105-PA	IPI00421711.1	2.58±NA	1	Q6PDU7	300677
Hypothetical protein LOC314432	IPI00368347.2	1.63±0.04	8	Q5U300	314432
Transporter or channel					
ADP/ATP translocase 2	IPI00200466.2	1.78±0.28	3	Q09073	25176
ATPase, H+ transporting, V1 subunit E isoform 1	IPI00400615.1	1.63±1.16	2	Q6PCU2	297566

Table 1. Continued

Description	IPI ID	Average ratio Average±SD	Quantification Peptide Num	UniProtKB ID/AC	Gene ID
Cationic amino acid transporter-1	IPI00190498.1	1.81±NA	1	Q8VIA9	25648
Fragile X mental retardation gene 1, autosomal homolog	IPI00373184.2	3.19±0.34	3	Q5XI81	361927
Mitochondrial 2-oxoglutarate/malate carrier protein	IPI00231261.6	1.97±NA	1	P97700	64201
Na-K-Cl cotransporter	IPI00212590.1	2.34±NA	1	Q9QX10	83629
Nuclear protein localization protein 4 homolog	IPI00191492.2	1.51±NA	1	Q9ES54	140639
PREDICTED: secretory carrier membrane protein 3	IPI00206037.5	1.52±NA	1	Q9ERM8	65169
PREDICTED: similar to ATPase, H+ transporting, V1 subunit A, isoform 1	IPI00373076.1	1.86±0.41	2		360716
PREDICTED: similar to importin 7	IPI00206234.2	1.89±0.62	3		308939
PREDICTED: similar to p59 immunophilin	IPI00358443.2	1.59±NA	1	Q8K3U8	260321
PREDICTED: similar to tweety homolog 2	IPI00361325.2	3.49±NA	1		287803
Rho/rac guanine nucleotide exchange factor	IPI00368617.2	1.66±0.05	3	Q5FVC2	310635
Sideroflexin-1	IPI00213735.2	9.59±NA	1	Q63965	364678
Similar to SEC24 related gene family, member	IPI00365299.2	1.55±0.21	3		685144
Slc25a3 protein	IPI00209115.2	2.51±0.03	5	Q6IRH6	245959
Sodium- and chloride-dependent taurine transporter	IPI00327953.2	2.67±0.07	2	P31643	29464
Splice Isoform SERCA2B of Sarcoplasmic/ endoplasmic reticulum calcium ATPase 2	IPI00190020.3	2.20±0.00	2	Q71UZ2	29693
Splice Splice Isoform IIBA of Dynamin-2	IPI00210319.2	1.59±NA	1	P39052	25751
Vacuolar ATP synthase subunit B, brain isoform	IPI00199305.1	1.96±0.11	5	P62815	117596
Vacuolar ATP synthase subunit F	IPI00198291.1	1.67±NA	1	P50408	116664
PREDICTED: similar to peroxisomal integral membrane protein	IPI00366455.1	1.86±NA	1		300083
Cell cycle, cell proliferation and differentiation					
Casein kinase II subunit alpha	IPI00192586.1	1.69±NA	1	P19139	116549
NG,NG-dimethylarginine dimethylaminohydrolase 1	IPI00231194.4	1.81±NA	1	O08557	64157
Nucleosome assembly protein 1-like 4	IPI00366110.3	1.53±0.05	2		361684
PREDICTED: similar to cullin 4A	IPI00364684.2	1.61±NA	1		361181
PREDICTED: similar to hepatic multiple inositol polyphosphate phosphatase	IPI00364031.1	2.69±0.00	2		499084
Single-stranded DNA-binding protein, mitochondrial precursor	IPI00196750.1	1.82±0.20	2	P28042	54304
Others and molecular function unclassified					
37 kDa protein	IPI00562745.1	2.94±NA	1		
9 kDa protein	IPI00567137.1	2.28±0.77	2		
Coiled-coil domain-containing protein 47 precursor	IPI00203647.1	1.92±0.00	2	Q5U2X6	303606
Cold shock domain-containing protein E1	IPI00190971.1	1.62±0.00	2	P18395	117180
Complement component 1, Q subcomponent-binding protein, mitochondrial precursor	IPI00361686.4	2.26±0.15	4	O35796	29681
Cysteine-rich with EGF-like domain protein 1 precursor	IPI00202520.1	2.87±NA	1	Q4V7F2	312638
FK506-binding protein 9 precursor	IPI00215190.1	1.57±0.00	2	Q66H94	297123
Hypothetical protein	IPI00389960.2	1.87±NA	1	Q5XI01	686883
Hypothetical protein LOC498174	IPI00394488.2	1.84±NA	1	Q5RK08	498174
Hypothetical protein RGD1306649	IPI00197896.1	2.46±0.20	2	Q4FZT8	288772
Kidney predominant protein NCU-G1	IPI00196226.1	1.55±0.00	2	Q68FV6	295231
LOC500199 protein	IPI00204675.4	1.60±NA	1	Q4KM70	500199
Major vault protein	IPI00231381.7	1.92±0.03	2	Q62667	64681
Myeloid-associated differentiation marker	IPI00339007.1	2.17±NA	1	Q6VBQ5	369016
N-acylsphingosine amidohydrolase 1	IPI00421601.3	1.81±0.02	2	Q9EQJ6	84431
Nicalin precursor	IPI00369465.2	2.15±NA	1	Q5XIA1	314648
Nucleolar protein 3	IPI00209297.1	2.35±0.08	2	Q62881	85383
O-GlcNAcase	IPI00208152.1	17.41±NA	1	Q8VIJ5	154968

Table 1. Continued

Description	IPI ID	Average ratio Average±SD	Quantification Peptide Num	UniProtKB ID/AC	Gene ID
Paraspeckle protein 1	IPI00203753.1	1.52±NA	1	Q4KLH4	305910
Peroxisomal biogenesis factor 11b	IPI00210003.1	2.31±NA	1	Q4KM24	310682
Pleckstrin homology domain containing, family C	IPI00362106.2	1.99±0.14	3	Q5XI19	289992
Poliovirus receptor	IPI00326594.11	8.10±NA	1		25066
PREDICTED: ATPase, H+ transporting, lysosomal accessory protein 2	IPI00358308.2	2.24±NA	1	Q6AXS4	302526
PREDICTED: similar to 0910001A06Rik protein	IPI00366405.2	1.87±0.00	2		299909
PREDICTED: similar to ARL6IP2	IPI00365499.3	2.17±NA	1	Q562A0	298757
PREDICTED: similar to C21ORF80	IPI00360543.2	1.79±0.00	2		309686
PREDICTED: similar to Coiled-coil-helix-coiled-coil-helix domain containing 6	IPI00364520.2	2.04±0.00	2		297436
PREDICTED: similar to collagen alpha 1(IV) chain precursor - mouse	IPI00362887.2	1.57±0.00	3	Q5FWY9	290905
PREDICTED: similar to GPI transamidase component PIG-T precursor	IPI00373349.1	1.50±0.00	2		296360
PREDICTED: similar to heparan sulfate proteoglycan 2	IPI00388323.4	2.33±0.21	24	Q62980	117511
PREDICTED: similar to Histidine triad nucleotide-binding protein 2	IPI00358757.2	1.81±0.00	2		313491
PREDICTED: similar to mKIAA0312 protein	IPI00196914.4	1.58±0.04	3	P51593	501546
PREDICTED: similar to NEDD9 interacting protein with calponin homology and LIM domains	IPI00371967.2	2.10±NA	1		294520
PREDICTED: similar to Pre-B-cell leukemia transcription factor interacting protein 1	IPI00201858.3	4.00±4.69	2	A2VD12	310644
PREDICTED: similar to RIKEN cDNA 0710008K08	IPI00210521.2	2.27±0.00	2		361185
PREDICTED: similar to RIKEN cDNA 5033414D02	IPI00209463.2	1.90±NA	1		293888
PREDICTED: similar to RIKEN cDNA 5730434I03 gene	IPI00364212.2	1.77±0.00	2		305284
PREDICTED: similar to signal recognition particle, 72 kDa subunit	IPI00565085.1	1.64±0.14	3		499086
PREDICTED: similar to Transcriptional activator protein PUR-alpha	IPI00197411.1	1.62±0.09	4		307498
Procollagen-lysine,2-oxoglutarate 5-dioxygenase 3 precursor	IPI00331772.4	1.97±0.22	3	Q5U367	288583
Proliferation related acidic leucine rich protein PAL31	IPI00192336.1	1.68±NA	1	Q9EST6	170724
Protein FAM98A	IPI00554081.1	1.73±NA	1	Q5FWT1	313873
Protein KIAA0152 precursor	IPI00371173.2	2.32±0.00	2	Q5FVQ4	304543
PTPRF interacting protein, binding protein 1 (liprin beta 1)	IPI00567984.1	1.63±0.00	2		312855
Reticulon 3, isoform A1	IPI00421506.1	1.64±0.20	4	A1L1I6	140945
Secreted acidic cysteine rich glycoprotein	IPI00557175.1	2.54±0.15	7	P16975	24791
Similar to PRUNEM1	IPI00368646.1	3.17±NA	1	Q6AYG3	310664
Splice Isoform 2 of Procollagen-lysine, 2-oxo-glutarate 5-dioxygenase 2 precursor	IPI00208888.1	1.74±0.32	4	Q811A3	300901
Tangerin	IPI00203791.2	4.55±NA	1	Q5PQM3	309169
Thymosin beta-10	IPI00231695.5	2.61±NA	1	P63312	50665
Transmembrane emp24 protein transport domain containing 9	IPI00364707.1	1.91±0.00	2	Q5I0E7	361207
Transmembrane protein 109 precursor	IPI00372499.1	2.21±NA	1	Q6AYQ4	361732
LOC360721 protein	IPI00608138.1	2.87±NA	1	Q4QQV3	360721
Up-regulated during skeletal muscle growth protein 5	IPI00202111.1	2.28±0.00	2	Q9JJW3	171069
WD-containing protein	IPI00205633.6	2.30±NA	1	Q9R037	246152

Table 2. The list of proteins with the ratio $\leq$0.5

Description	IPI ID	Average Ratio Average±SD	Quantification Peptide Num	UniProtKB ID/AC	Gene ID
Alcohol dehydrogenase class 4 mu/sigma chain	IPI00324743.1	0.38±0.03	3	P41682	171178
Amidophosphoribosyltransferase precursor	IPI00198619.1	0.43±NA	1	P35433	117544
APEX (Fragment)	IPI00200918.1	0.48±NA	1	Q99PF3	79116
Capping protein	IPI00464670.1	0.39±0.00	2	Q6AYC4	297339
CD14 antigen	IPI00231949.5	0.24±NA	1	Q63691	60350
Galectin-3	IPI00194341.4	0.44±0.01	5	P08699	83781
Glutaredoxin-1	IPI00231191.6	0.49±0.07	2	Q9ESH6	64045
Mevalonate kinase	IPI00214563.1	0.20±NA	1	P17256	81727
Minichromosome maintenance protein 7	IPI00371012.2	0.49±0.07	4	Q1PS21	288532
Mtap6 protein (Fragment)	IPI00212447.2	0.31±NA	1	Q6AYX8	29457
N-myc downstream regulated gene 1	IPI00421389.1	0.38±NA	1	Q6JE36	299923
NORBIN	IPI00205396.1	0.44±NA	1	O35095	89791
Pleckstrin homology-like domain, family B, member 1	IPI00207827.2	0.36±NA	1	Q63312	171434
PREDICTED: cadherin 11	IPI00211883.2	0.43±0.02	2	Q9JIW2	84407
PREDICTED: similar to 2610304F09Rik protein	IPI00358454.2	0.46±0.00	2		307527
PREDICTED: similar to cCoronin, actin binding protein 1C	IPI00388015.3	0.33±0.46	3	B2RYG0	501841
PREDICTED: similar to DNA replication licensing factor MCM3	IPI00361669.2	0.44±NA	1		367976
PREDICTED: similar to DNA replication licensing factor MCM3	IPI00371781.2	0.44±NA	1		316273
PREDICTED: similar to Filamin B	IPI00373752.2	0.47±0.12	6		306204
PREDICTED: similar to Lmnb2 protein	IPI00366190.3	0.42±NA	1		299625
PREDICTED: similar to stromal cell-derived factor 2 precursor	IPI00369655.1	0.38±NA	1		287470
PREDICTED: similar to TF-1 apoptosis related protein 19	IPI00193547.2	0.33±NA	1		292814
PREDICTED: similar to Tripartite motif protein 47	IPI00361534.1	0.3±NA	1		690374
PREDICTED: similar to Williams-Beuren syndrome deletion transcript 9 homolog	IPI00370333.1	0.29±NA	1	Q2V6G6	368002
Prostaglandin F2 receptor negative regulator p recursor	IPI00208280.2	0.47±0.27	3	Q62786	29602
Prostaglandin-endoperoxide synthase 1	IPI00567836.1	0.48±0.01	3	Q66HK3	24693
Proteasome inhibitor PI31 subunit	IPI00391791.2	0.27±NA	1	Q5XIU5	682071
Reck reversion-inducing-cysteine-rich protein with kazal motifs	IPI00358750.2	0.48±NA	1		313488
Ribonucleotide reductase M1	IPI00361151.2	0.47±NA	1	Q5U2Q5	365320
RNA terminal phosphate cyclase domain 1	IPI00201443.1	0.37±NA	1	Q68FS8	295395
RNA-binding motif protein 3	IPI00367437.3	0.50±0.00	2	Q925G0	114488
Small nuclear ribonucleoprotein polypeptide A	IPI00364044.3	0.20±0.00	2	Q5U214	292729
Testis derived transcript	IPI00560148.2	0.4±NA	1	Q2LAP6	500040
Transcriptional repressor CTCF	IPI00207172.2	0.47±NA	1	Q9R1D1	83726
UDP-glucose 6-dehydrogenase	IPI00195803.1	0.44±0	2	O70199	83472
Wiskott-Aldrich syndrome protein-interacting protein	IPI00470232.5	0.3±NA	1	Q6IN36	117538
Xanthine dehydrogenase/oxidase	IPI00231694.6	0.50±0.07	3	P22985	497811

folding, cell adhesion and extracellular matrix, cell structure and motility, metabolism, substance transportation, etc. These patterns of up-regulation were consistent with the functional and structural characteristics of skeletal muscle cells. To explore functional modules of the proteins we quantified, protein interaction network was predicted by STRING (see Supporting Information Fig. 2).

3.3.1 Mediators of signaling pathway

Myogenic differentiation is regulated by positive and negative signals from surroundings. After switching the cells from nutrient-rich media to nutrient-poor medium by lowering FBS content from 10 to 2%, L6 myoblasts are able to sense the physical and chemical signals of lowered FBS

through specific membrane receptors [2]. Once L6 myoblasts sense these signals, a series of intracellular events will be triggered. The result of these events is the increased expression of MyoD and myogenin. MyoD and myogenin initiate multiple muscle differentiation-specific genes transcription for myogenic process [1, 2]. Although the role of mitogen-activated protein kinase (MAPK) signaling cascades in myogenesis is controversial, accumulating studies have shown that MAPK is activated during the differentiation of myogenic cell lines and is essential for the expression of muscle-specific genes [15, 16]. Activation of MAPK signaling cascades in myoblasts can modulate the activity of MyoD establishing dynamic modulation of the MyoD-induced programs of gene expression [3]. We observed that terminally differentiated myotubes increase the expression of some MAPK-pathway associated proteins, for example, Map4k4, MAPKK 1, etc. However, the amount of most MAPK remains stable, because they are modified as functional executors at different stages of differentiation [17]. A kinase anchor protein 2, exhibiting binding protein kinase A and being involved in actin filament organization, protein localization and the transmembrane receptor protein serine/threonine kinase signaling pathway, was also found up-regulated. Interestingly, prohibitin (PHB), a ubiquitously expressed and evolutionarily highly conserved protein, was found up-regulated once myoblasts initiated differentiation. This result is supported by Western blot data (Fig. 2b) and the results of Tannu [6]. PHB has been found to be presented in the nucleus, the mitochondria and the plasma membrane. Gamble *et al.* [18, 19] reported that PHB participated in the activation of the Raf-MEK-ERK pathway. Sun and colleagues [20] reported that PHB-2 could repress muscle differentiation by inhibiting MyoD and MEF2 in C2C12 cells. From these clues, prohibitin may belong to MAPK cascade and play important role in muscle differentiation. Besides MAPK-related factors, we also found some other signaling molecules that were up-regulated in muscle cells, such as inositol 1, 4, 5-triphosphate receptor 3 (IP3R-3), latent transforming growth factor beta-binding protein 1 (LTBP-1), phosphatidylethanolamine-binding protein, SH2-containing inositol phosphatase 2 (SHIP2), and guanine nucleotide-binding protein G (i), alpha-2, *etc*. IP3R-3, in connection with acetylcholine signaling, adrenergic signaling, endothelin signaling, PDGF signaling, chemokine and cytokine signaling and Wnt signaling *etc*. is the receptor for inositol 1,4,5-trisphosphate mediating the release of intracellular calcium. The alteration of IP3R-3 abundance in muscle may be to match the excitation-contraction coupling of muscle cell. LTBP-1 targets latent complexes of transforming growth factor beta to the extracellular matrix. It interacts with architectural extracellular matrix macromolecules—fibrillins that form ubiquitous extracellular microfibril suprastructures in the connective tissue space. But, it is unknown whether LTBP-1 participates in myogenic initiation and myoblast fusion [21, 22]. In addition, we found one non-muscle differentiation-promoting protein, transcriptional activator protein Pur beta, was up-regulated by 3.76-fold in myotubes. This protein is known to regulate myeloid cell differentiation. It remains unclear how this protein functions in myogenic differentiation. In our study, many myogenesis-control factors, such as MyoD and myogenin, were not observed, probably because of very low abundance in the cells.

3.3.2 Protein synthesis-and degradation-related proteins

Synthesis of muscle-specific proteins increases significantly during the myogenic process. Many proteins associated with proteins synthesis were found up-regulated in this study, including many amino acid-tRNA synthetases, eukaryotic translation elongation factors, eukaryotic translation initiation factors and ribosomal proteins. These types of proteins also have been reported in previous studies [6–9]. As protein synthesis and degradation is a finely coordinate process [23] some protein-degradation related proteins were observed up-regulated here. It is well known that the protein degradation system serves as a quality-control system for abnormal proteins to maintain cellular homeostasis [24]. Yet, as early as 1997, Gardrat [25] hypothesized that ubiquitin-proteasome pathway was involved in muscle-cell differentiation. In 2005, Schwartz group [26] discovered that both MyoD and inhibitor of DNA binding 1(Id1) are rapidly degraded by the ubiquitin-proteasome pathway during the differentiation of myoblast to myotube in mouse C2C12 myoblast cells, but the reduction of Id1 is more than MyoD markedly. Rapid reduction of Id1 can release repression on MyoD, and then MyoD will trigger muscle-specific gene transcription. This shows that ubiquitin-proteasome pathway is essential to initiation of mygenic differentiation by controlling muscle differentiation-specific gene expression [26]. Proteasomes, performing ATP-dependent proteolysis, are large protein complexes formed by many subunits. In this study, we found that many proteasomal proteins, such as PSMA1, PSMA2, PSMA3, PSMA4, PSMA5, PSMB1, PSMB2, PSMD2, PSMD3, the 26S protease regulatory subunit 7 and 26S protease regulatory subunit 4, were up-regulated during myogenic process. From the STRING network view, it can be seen directly that these proteins have the strong interactions (Supporting Information Fig. 2). Obviously, the changes of proteolytic system we found support the theory of myogenesis addressed by preceding publications [25, 26].

3.3.3 Molecular chaperone

Molecular chaperones are a group of proteins whose roles are to assist newly translated proteins to fold properly as functional mature proteins or lead the misfolded proteins to degradation mentioned above. In differentiating muscle cells, the single nascent myosin molecule must go through folding and assemble into motor thick filament with associated proteins. It has been reported that Hsp90 and Hsc70 form a complex with newly synthesized myosin and these

chaperones promote myofibril assembly [27]. In this study, Hsp90, Hsc70 (heat shock cognate 71-kDa protein), Hsc70-interacting protein, have been up-regulated by 1.50-, 1.58- and 1.83-fold, respectively in L6 myotube cells. In addition, glucose-regulated protein precursor, hypoxia up-regulated 1 and heat shock 70-kDa protein 4, belonging to Hsp70 family chaperone, were also up-regulated in our study. It has been proved by Western blot that Hsp70 were increased during differentiation of myotubes [28]. T-complex protein 1 subunit alpha (TCP-1-alpha or CCT-alpha), a molecular chaperone of actin and tubulin, has also been found to be up-regulated by 1.7-fold. Its CCT activity is required for cell-cycle progression and cytoskeleton organization in mammalian cells [29]. In this study, we also identified some small heat shock proteins, such as HspB1 (Hsp27), HspB8 (Hsp22), and aB-crystallin. These proteins can confer resistance to apoptosis during myogenic differentiation [30]. In addition, Hsp27 controlled by P38/MAPK pathway can modify actin polymerization. These behaviors of such proteins are beneficial to myogenic differentiation. Hsp27 and Hsp22 were up-regulated 2.55- and 2.09-fold, respectively. Alpha B-crystallin also has important effect on myotubes development. This protein was identified in our experiment with no quantified SILAC ratio. However, the MS spectra intensities of some light/heavy peptide pairs of αB-crystallin checked manually has confirmed its up-regulation in myotubes (data not shown). In summary, the observed up-regulated molecular chaperones of cytoskeleton proteins play an important role in muscle differentiation.

3.3.4 Cell-adhesion proteins

Myoblasts-myotubes conversion requires cell-cell mutual interaction and fusion between myoblasts. No doubt, adhesion molecules must be involved in this process. Some cell-adhesion molecules have been reported to be involved in controlling the fusion of myoblasts during muscle development [31, 32]. Grossi and colleagues [33] have shown that mechanical stimulation can promote C2C12 cells differentiation through the laminin receptor. In this study, many extracellular matrix linker proteins were identified and showed increased expression in the L6 terminal differentiation stage, such as integrin beta-1 precursor (2.3-fold), isoform 1 of fibronectin precursor (2.3-fold), splice isoform 2 of fibronectin precursor (2.3-fold), procollagen C-proteinase enhancer protein (2.44-fold), protein-lysine 6-oxidase precursor (2.56-fold), splice isoform short of collagen alpha-1(XII) chain (1.73-fold) and vinculin (1.55-fold). These proteins are involved in cell adhesion, cell communication, cell motility, and maintenance of cell shape. Integrin beta-1 is a subunit of several integrin proteins. Integrin is a receptor for fibronectin, collagen, and laminins. Brzoska [34] has shown that integrin α3 subunit participates in myoblast adhesion and fusion *in vitro*. When α3β1 integrin binds to its ligands, intracellular signaling is triggered, and then elicits cytoskeleton reorganization to keep cell adhesion, cell motility and cell shape. Integrin also drives Raf/MEK/ERK pathway [35]; from this point of view, myoblast cell-to-cell adhesion might act as a trigger to initiate the transcription of muscle-specific genes. It is reasonable that enhanced expression of these proteins in terminally differentiated myocytes strengthened cell-cell, cell-matrix adhesion and provided physical stabilization and tenacity against the tensile forces generated during muscle contraction.

3.3.5 Cell structure and motility-associated proteins

Skeletal myogenic differentiation involved in extensive changes in cell morphology and subcellular architectures. During the differentiation process, myoblasts fuse to form multinucleated myotubes. This morphological change reflects a massive structural reorganization of cytoplasmic components including subcellular organelles [36]. Two dynamic filament systems, microtubules and microfilaments, have been considered to participate actively in generating the spatial organization of the cell [37]. Realignment of nascent α-actin and myosin into sarcomeres of myofibrils depended on microtubules network reorganization [37]. Responding to this cell-shape change, many cytoskeleton proteins are up-regulated in L6 myotubes, for instance, microtubule-associated proteins, actin-related protein 2/3 complex subunit 1A (Arpc1a), transgelin, dynamin-2 and kinesin-1 etc. Microtubule-associated protein 4 is found to be required for myogensis. Antisense inhibition of muscle-specific microtubule-associated protein-4 during differentiation severely perturbed myotube formation, but had no effect on growth and cell fusion [38]. Actin-related protein 2/3 formed complex with WASP or WAVE protein to mediate the actin polymerization and the formation of branched actin networks. Transgelin, an actin cross-linking/gelling protein, is also up-regulated 4.90-fold. Dynamin-2, a microtubule-associated force-producing protein involved in producing microtubule bundles and vesicular trafficking processes [39], may be also associated with myoblasts fusion. Kinesin-1, a microtubule-dependent motor required for normal distribution of cellular components, was up-regulated by 4.4-fold, which indicates that myotube is a critical dynamic cellular component in myoblast differentiation [40]. Besides microtubules, intermediate filament is another important family of cytoskeletal proteins associated with myotubes transformation. Muscle-specific intermediate filaments (IF) include desmin, nestin, vimentin and other [41, 42]. These proteins are synthesized by muscle cells depending on the type of muscle and its stage of development. Desmin is presented in all muscles at all stages of development and the others appear transiently or in only certain muscles [41, 42]. In our experiment, desmin was identified but its relative expression ratio in myotubes compared to myoblast was not showed by Census software. However, Western blot result shows that the expression of desmin was up-regulated along with myogenic process. Our

SILAC data show that nestin is highly up-regulated in day 4 L6 myotubes (7.23-fold). It is well known that nestin is a crucial component in neuron differentiation, but it is less clear how nestin functions during myogenic development.

Once myocytes form, muscle-specific contractile proteins also highly express. Skeletal muscle actin α, a basic component of thin filament, was up-regulated 2-fold. Myosins are actin-based motor proteins and the main component of thick filament. Myosin heavy chain (MHC), a myotube-specific marker, was up-regulated 220-fold. Myosin heavy polypeptide 2 and myosin light polypeptide 4 also were found increased intensely in L6 myotubes comparing to myoblasts. Splice isoform 1 of tropomyosin 1 alpha and splice isoform 2 of tropomyosin beta increased by up to about 2-fold compared to myoblasts. Tropomyosins can bind to actin filaments and associate with the troponin complex to regulate muscle contraction in a calcium-dependent manner.

Taken together, all of these observations are consistent with the muscle contractility. The up-regulation of microtubule, intermediate filament and microfilament can facilitate reframed-shape of myotubes during myogensis and maintain the structural and functional integrity of skeletal muscle.

3.3.6 Metabolism-related proteins

Because skeletal muscle is force-producing contractile machinery, various metabolic events, such as ATP production, are very active during skeletal muscle contraction. In myotubes, there is an extreme demand for ATP for muscle contraction and ATP-dependent calcium signaling. To meet this demand, skeletal muscle metabolizes large amount of glucose, fatty acids and amino acids to produce energy [43]. Consistent with this, myotubes express a large number of proteins and enhance mitochondrial function to metabolize the energy-providing products. In this study, we identified 92 proteins whose expression increased at least 1.5-fold and have been annotated to be related to energy metabolism. Among this type of proteins, 24 proteins were mapped to glucose metabolism, 19 proteins to fatty acid metabolism, 21 proteins to oxidative phosphorylation/electron transport, 13 proteins to amino acid metabolism, and 24 proteins to other metabolic functions. For example, the expression level of glyceraldehyde-3-phosphate dehydrogenase increased 2.76-fold, long-chain fatty acid-CoA ligase 14.26-fold, fructose-bisphosphate aldolase A 3.16-fold, pyruvate dehydrogenase beta 2.91-fold, mitochondrial malate dehydrogenase 2.04-fold, citrate synthase 2.1-fold, all of which being consistent with Ong's results [8]. ATP synthase B chain, ATP synthase D chain, ATP synthase beta chain and ATP synthase delta chain, the enzymes for oxidative phosphorylation, have increased significantly. GADPH, a housekeeping protein, is usually used as a control for relative protein quantification by Western blot. In this study, cells increase GADPH expression from the start of differentiation (Fig. 2B), but GADPH expression was down-regulated after 4 days starvation (day 8) because of a decrease in glycolysis. In contrast to the Western blot results for other proteins, the decreasing expression of GADPH at day 8 suggests that GADPH may not be dominant factor in differentiation.

3.3.7 Transporters or channel proteins

Consistent with excitable and contractile characteristic of muscle, some transporters or channel proteins are highly expressed in myotubes. Skeletal muscle cells are stimulated by acetylcholine released at neuromuscular junctions by motor neurons. Ion Na^+ flow into cell by Na^+-K^+ transporters and subsequently cells produce action potentials. Once the cells are excited, their sarcoplasmic reticulums release Ca^{2+} through sarcoplasmic/endoplasmic reticulum calcium ATPase. Ca^{2+} interacts with the myofibrils and induces muscular contraction. During muscular contraction, cells consume a mass of ATP and produce substantive H^+. Moreover, increase of ion Ca^{2+} could enhance myoblasts differentiation during the myogenic process [44]. These substrates need the help of ion transporters to pass through the cytoplasmic membranes. To meet these needs, ionic sodium, potassium, calcium, hydrogen transporter and cationic amino acid transporter were highly expressed in finally differentiated cell.

Among the proteins with the expression ratio of <0.5 (Table 2), some have been shown to be associated with myogenic process, such as prostaglandin F2 receptor negative regulator (PTGFRN) and prostaglandin-endoperoxide synthase 1 (COX-1). PTGFRN can inhibit the effect of PG F2 by binding to PG F2 receptor. COX-1 is a rate-control enzyme of PG synthesis. Many studies have shown that PG including PG F2 can promote the myogenesis by different ways [45]. If it is the case, down-regulation of PGF2 receptor negative regulator can facilitate the positive effect of PG F2 on myogenic process. However, down-regulation of COX-1 looks controversial to this case. Yet, Bondesen [46] showed recently that PG I2 could inhibit myogenesis *in vitro* by blocking myoblast migration and fusion. These data indicate that there are still some controversies in myogenesis and more detailed investigations are needed.

4 Concluding remarks

SILAC based quantitative proteomic approach was successfully applied to analyze skeletal-muscle differentiation. In this study, owing to isotopic arginine labeling SILAC approach was used, therefore, only tryptic peptides with arginine carboxyl-terminal could be used for quantification. Suppose isotopic arginine and lysine double labeling SILAC approach would improve the accuracy of protein quantification and increase the number of peptides/proteins quantified. From our data, most of the up- or down-regulated proteins we quantified in the terminally differentiated L6 cells may provide principal or accessory support for the myogen-

esis process. Proteins whose expression remained unchanged during differentiation suggest that alternate mechanisms, such as modification or interactions, may be involved in muscle differentiation. For example, MAPK1 and β-catenin are the pivotal nodes of the signaling pathway that play an important role in the myogenic process. Further experiments are required to elucidate their roles in more details. Overall, SILAC was effective in elucidating the molecular mechanisms of skeletal-muscle differentiation in this study, and our data present more clues on myogenic development. As mentioned at the very beginning of this article, skeletal-muscle differentiation is a very complicated and dynamic process that is controlled spatio-temporally by multifarious types of factors at different transcriptional levels. The transcriptions of most proteins are dynamic, depending on the type of muscle, its stage of development and the species. In our opinion, it will be essential and challenging in the future to systematically grasp the dynamic changes of different types of proteins and their appropriate integrated functions during skeletal-muscle differentiation.

This research was supported by the National Basic Research Program of China (973) (grant no. 2004CB720004) and the National Natural Science Foundation of China (grant no. 30670587, 30570466). JRY is supported by NIH P41 RR011823.

The authors have declared no conflict of interest.

5 References

[1] Wagers, A. J., Conboy, I. M., Cellular and molecular signatures of muscle regeneration: current concepts and controversies in adult myogenesis. *Cell* 2005, *122*, 659–667.

[2] Parker, M. H., Seale, P., Rudnicki, M. A., Looking back to the embryo: defining transcriptional networks in adult myogenesis. *Nat. Rev. Genet.* 2003, *4*, 497–507.

[3] Lluís, F., Perdiguero, E., Nebreda, A. R., Muñoz-Cánoves, P., Regulation of skeletal muscle gene expression by p38 MAP kinases. *Trends Cell. Biol.* 2006, *16*, 36–44.

[4] Aebersold, R., Mann, M., Mass spectrometry-based proteomics. *Nature* 2003, *422*, 198–207.

[5] Ong, S. E., Mann, M., Mass spectrometry-based proteomics turns quantitative. *Nat. Chem. Biol.* 2005, *5*, 252–262.

[6] Tannu, N. S., Rao, V. K., Chaudhary, R. M., Giorgianni, F. *et al.*, Comparative proteomes of the proliferating C(2)C(12) myoblasts and fully differentiated myotubes reveal the complexity of the skeletal muscle differentiation program. *Mol. Cell. Proteomics* 2004, *3*, 1065–1082.

[7] Gonnet, F., Bouazza, B., Millot, G. A., Ziaei, S. *et al.*, Proteome analysis of differentiating human myoblasts by dialysis-assisted two-dimensional gel electrophoresis (DAGE). *Proteomics* 2008, *8*, 264–278.

[8] Kislinger, T., Gramolini, A. O., Pan, Y., Rahman, K. *et al.*, Proteome dynamics during C2C12 myoblast differentiation. *Mol. Cell. Proteomics* 2005, *4*, 887–901.

[9] Ong, S. E., Blagoev, B., Kratchmarova, I., Kristensen, D. B. *et al.*, Stable isotope labeling by amino acids in cell culture, SILAC, as a simple and accurate approach to expression proteomics. *Mol. Cell. Proteomics* 2002, *1*, 376–386.

[10] Mann, M., Functional and quantitative proteomics using SILAC. *Nat. Rev. Mol. Cell. Biol.* 2006, *7*, 952–958.

[11] Delahunty, C., Yates, J. R. 3rd, Protein identification using 2D-LC-MS/MS. *Methods* 2005, *35*, 248–255.

[12] McDonald, W. H., Tabb, D. L., Sadygov, R. G., MacCoss, M. J. *et al.*, MS1, MS2, and SQT-three unified, compact, and easily parsed file formats for the storage of shotgun proteomic spectra and identifications. *Rapid Commun. Mass. Spectrom.* 2004, *18*, 2162–2198.

[13] Cociorva, D., Tabb, D. L., Yates, J. R. 3rd, Validation of tandem mass spectrometry database search results using DTASelect. In: *Curr. Protoc. Bioinformatics*. John Wiley & Sons Inc, New Jersey 2007, Chapter 13, Unit 13.4.

[14] Park, S. K., Venable, J. D., Xu, T., Yates, J. R. 3rd, A quantitative analysis software tool for mass spectrometry-based proteomics. *Nat. Methods* 2008, *5*, 319–322.

[15] Bennett, A. M., Tonks, N. K., Regulation of distinct stages of skeletal muscle differentiation by mitogen-activated protein kinases. *Science* 1997, *278*, 1288–1291.

[16] Keren, A., Tamir, Y., Bengal, E., The p38 MAPK signaling pathway: a major regulator of skeletal muscle development. *Mol. Cell. Endocrinol.* 2006, *252*, 224–230.

[17] Gredinger, E., Gerber, A. N., Tamir, Y., Tapscott, S. J., Bengal, E., Mitogen-activated protein kinase pathway is involved in the differentiation of muscle cells. *J. Biol. Chem.* 1998, *273*, 10436–10444.

[18] Gamble, S. C., Chotai, D., Odontiadis, M., Dart, D. A. *et al.*, Prohibitin, a protein downregulated by androgens, represses androgen receptor activity. *Oncogene* 2007, *26*, 1757–1768.

[19] Rajalingam, K., Wunder, C., Brinkmann, V., Churin, Y. *et al.*, Prohibitin is required for Ras-induced Raf-MEK-ERK activation and epithelial cell migration. *Nat. Cell Biol.* 2005, *7*, 837–843.

[20] Sun, L., Liu, L., Yang, X. J., Wu, Z., Akt binds prohibitin 2 and relieves its repression of MyoD and muscle differentiation. *J. Cel. Sci.* 2004, *117*, 3021–3029.

[21] Isogai, Z., Ono, R. N., Ushiro, S., Keene, D. R. *et al.*, Latent transforming growth factor beta-binding protein 1 interacts with fibrillin and is a microfibril-associated protein. *J. Biol. Chem.* 2003, *278*, 2750–2757.

[22] Hubmacher, D., Tiedemann, K., Reinhardt, D. P., Fibrillins: from biogenesis of microfibrils to signaling functions. *Curr. Top. Dev. Biol.* 2006, *75*, 93–123.

[23] Gustavo, A., Nader Molecular determinants of skeletal muscle mass: getting the "AKT" together. *Int. J. Biochem. Cell Biol.* 2005, *37*, 1985–1996.

[24] Goldberg, A. L., Protein degradation and protection against misfolded or damaged proteins. *Nature* 2003, *426*, 895–899.

[25] Gardrat, F., Montel, V., Raymond, J., Azanza, J. L., Proteasome and myogenesis. *Mol. Biol. Rep.* 1997, *24*, 77–81.

[26] Sun, L., Trausch-Azar, J. S., Ciechanover, A., Schwartz, A. L., Ubiquitin-proteasome- mediated degradation, intracellular

localization, and protein synthesis of MyoD and Id1 during muscle differentiation. *J. Biol. Chem.* 2005, *280*, 26448–26456.

[27] Srikakulam, R., Winkelmann, D. A., Chaperone-mediated folding and assembly of myosin in striated muscle. *J. Cell Sci.* 2004, *117*, 641–652.

[28] Ito, H., Kamei, K., Iwamoto, I., Inaguma, Y., Kato, K., Regulation of the levels of small heat-shock proteins during differentiation of C2C12 cells. *Exp. Cell. Res.* 2001, *266*, 213–221.

[29] Grantham, J., Brackley, K. I., Willison, K. R., Substantial CCT activity is required for cell cycle progression and cytoskeletal organization in mammalian cells. *Exp. Cell Res.* 2006, *312*, 2309–2324.

[30] Kamradt, M. C., Chen, F., Sam, S., Cryns, V. L., The small heat shock protein alpha B-crystallin negatively regulates apoptosis during myogenic differentiation by inhibiting caspase-3 activation. *J. Biol. Chem.* 2002, *277*, 38731–38736.

[31] Covault, J., Sanes, J. R., Distribution of N-CAM in synaptic and extrasynaptic portions of developing and adult skeletal muscle. *J. Cell Biol.* 1986, *102*, 716–730.

[32] Levi, G., Cell adhesion molecules during Xenopus myogenesis. *Cytotechnology* 1993, *11*, s91–93.

[33] Grossi, A., Yadav, K., Lawson, M. A., Mechanical stimulation increases proliferation, differentiation and protein expression in culture: Stimulation effects are substrate dependent. *J. Biomech.* 2007, *40*, 3354–3362.

[34] Brzoska, E., Bello, V., Darribere, T., Moraczewski, J., Integrin alpha3 subunit participates in myoblast adhesion and fusion *in vitro*. *Differentiation* 2006, *74*, 105–118.

[35] Johnson, G. L., Lapadat, R., Mitogen-activated protein kinase pathways mediated by ERK, JNK, and p38 protein kinases. *Science* 2002, *298*, 1911–1912.

[36] Squire, J. M., Architecture and function in the muscle sarcomere. *Curr. Opin. Struct. Biol.* 1997, *7*, 247–257.

[37] Pizon,V., Gerbal, F., Diaz, C. C., Karsenti, E., Microtubule-dependent transport and organization of sarcomeric myosin during skeletal muscle differentiation. *EMBO J.* 2005, *24*, 3781–3792.

[38] Mangan, M. E., Olmsted, J. B., Muscle-specific variant of microtubule-associated protein 4 (MAP4) is required in myogenesis. *Development* 1996, *122*, 771–781.

[39] Kessels, M. M., Dong, J., Leibig, W., Westermann, P., Qualmann, B., Complexes of syndapin II with dynamin II promote vesicle formation at the trans-Golgi network. *J. Cell Sci.* 2006, *119*, 1504–1516.

[40] Ginkel, L. M., Wordeman, L., Expression and partial characterization of kinesin related proteins in differentiating and adult skeletal muscle. *Mol. Biol. Cell* 2000, *11*, 4143–4158.

[41] Vaittinen, S., Lukka, R., Sahlgren, C., Hurme, T. *et al.*, The expression of intermediate filament protein nestin as related to vimentin and desmin in regenerating skeletal muscle. *J. Neuropathol. Exp. Neurol.* 2001, *60*, 588–597.

[42] Paulin, D., Xue, Z., *Desmin and Other Intermediate Filaments in Normal and Diseased Muscle*. Landes Bioscience and Springer US Press, Austin 2006, pp. 1–9.

[43] Richardson, R. S., Oxygen transport and utilization: an integration of the muscle systems. *Adv. Physiol. Educ.* 2003, *27*, 183–191.

[44] Porter, G. A., Makuck, R. F., Rivkees, S. A., Reduction in intracellular calcium levels inhibits myoblast differentiation. *J. Biol. Chem.* 2002, *277*, 28942–28947.

[45] Horsley, V., Pavlath, G. K., Prostaglandin F2 (alpha) stimulates growth of skeletal muscle cells via an NFATC2-dependent pathway. *J. Cell Biol.* 2003, *161*, 111–118.

[46] Bondesen, B. A, Jones, K. A., Glasgow, W. C., Pavlath, G. K., Inhibition of myoblast migration by prostacyclin is associated with enhanced cell fusion. *FASEB J.* 2007, *21*, 3338–3345.

